Supplementary Information

for

Evaluation of the pK_a's of Quinazoline Derivatives : Usage of Quantum Mechanical Based Descriptors

Melisa Kiran[1, ‡], Zeynep Pinar Haslak[1,2, ‡], Halit Ates[1], Viktorya Aviyente[1,*], Fatma Ahu Akin[1,*]

[1] Bogazici University, Department of Chemistry, 34342, Bebek, Istanbul, Turkey

[2] Université de Reims Champagne-Ardenne, 51687, Reims, France

Correspondance: akin@boun.edu.tr, aviye@boun.edu.tr

[‡]These authors contributed equally.

List of Figures

List of Tables

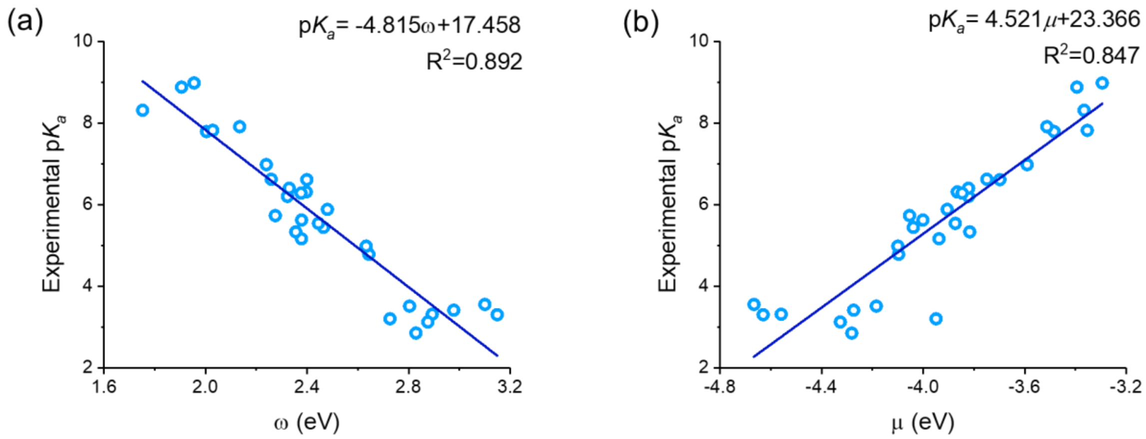

Figure S1. Linear regression between experimental pK_a and (a) calculated electrophilicity index (ω) and (b) calculated chemical potential (μ) at M06L/6-311++G(d,p) level of theory with CPCM solvation model.

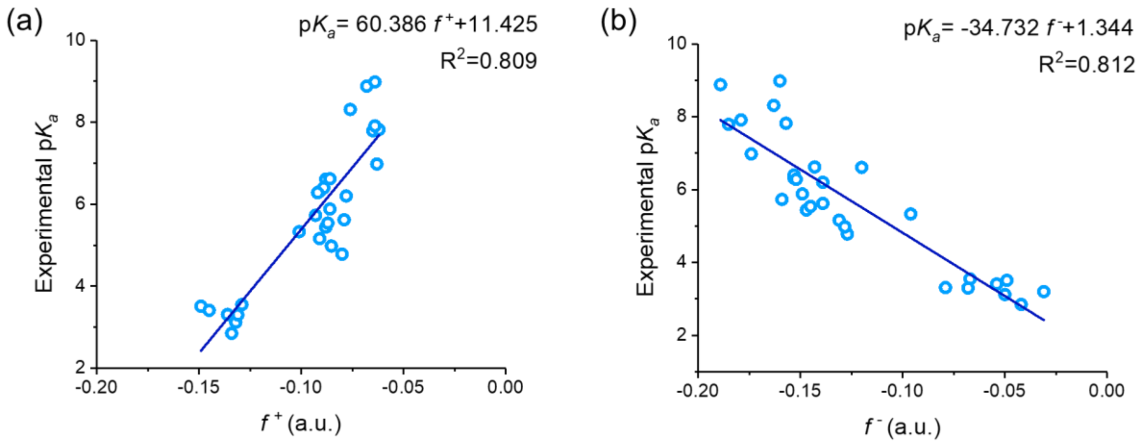

Figure S2. Linear regression between experimental pK_a and calculated (a) nucleophilic fukui function (f^+) and (b) electrophilic fukui function (f^-) on N_1 atom at M06L/6-311++G(d,p) level of theory with CPCM solvation model.

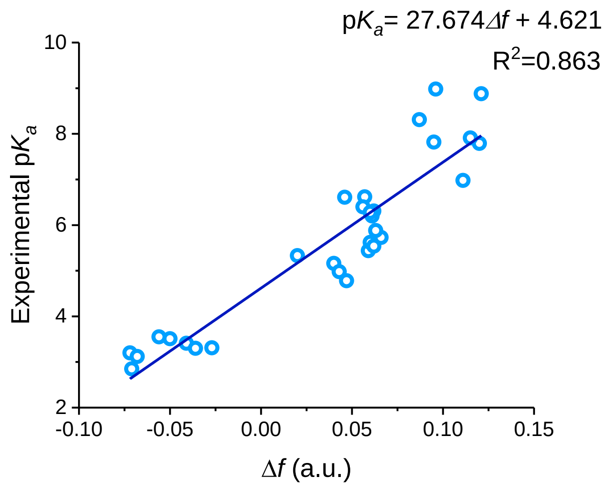

Figure S3. Linear regression between experimental pK_a and calculated condensed dual function (Δf = max{Δf (N_1), Δf(N_3)}) at M06L/6-311++G(d,p) level of theory with CPCM solvation model.

Table S1: Statistics for the quinazoline derivatives training set: R^2, MAD and MAX-ΔpK_a for different DFT methods, basis sets and solvation models using the Q = $q(N_1)$ atomic charge descriptor.

DFT/Basis Set	**Solvation Model**	**R^2**	**MAD**	**MAX-ΔpK_{as}**
M06L/6-31+G(d)	SMD	0.900	0.47	-1.41
M06L/6-311++G(d,p)	SMD	0.930	0.40	1.05
M06L/6-31+G(d)	CPCM	0.915	0.41	-1.24
M06L/6-311++G(d,p)	CPCM	0.927	0.40	0.96
M062X/6-31+G(d)	SMD	0.864	0.54	-1.58
M062X /6-311++G(d,p)	SMD	0.890	0.47	-1.40
M062X /6-31+G(d)	CPCM	0.874	0.50	-1.56
M062X /6-311++G(d,p)	CPCM	0.900	0.45	-1.26
B3LYP/6-31+G(d)	SMD	0.874	0.53	-1.56
B3LYP /6-311++G(d,p)	SMD	0.904	0.45	-1.27
B3LYP /6-31+G(d)	CPCM	0.898	0.46	-1.18
B3LYP /6-311++G(d,p)	CPCM	0.914	0.47	-1.48
ωB97XD/6-31+G(d)	SMD	0.876	0.53	-1.51
ωB97XD /6-311++G(d,p)	SMD	0.902	0.45	-1.30
ωB97XD /6-31+G(d)	CPCM	0.893	0.47	-1.52
ωB97XD /6-311++G(d,p)	CPCM	0.895	0.47	-1.24
MN12SX/6-31+G(d)	SMD	0.865	0.56	1.60
MN12SX /6-311++G(d,p)	SMD	0.885	0.48	-1.49
MN12SX /6-31+G(d)	CPCM	0.864	0.51	-1.52
MN12SX /6-311++G(d,p)	CPCM	0.896	0.47	-1.36

Table S2: Statistics for the quinazoline derivatives training set: R^2, MAD and MAX-ΔpK_a for different DFT methods, basis sets and solvation models using the Q = $q(N_3)$ atomic charge descriptor.

DFT/Basis Set	**Solvation Model**	**R^2**	**MAD**	**MAX-ΔpK_a**
M06L/6-31+G(d)	SMD	0.835	0.57	-1.77
M06L/6-311++G(d,p)	SMD	0.816	0.60	-1.90
M06L/6-31+G(d)	CPCM	0.864	0.50	-1.67
M06L/6-311++G(d,p)	CPCM	0.822	0.60	-1.65
M062X/6-31+G(d)	SMD	0.780	0.65	-2.13
M062X /6-311++G(d,p)	SMD	0.789	0.63	-2.19
M062X /6-31+G(d)	CPCM	0.809	0.61	-2.05
M062X /6-311++G(d,p)	CPCM	0.816	0.58	-2.03
B3LYP/6-31+G(d)	SMD	0.794	0.60	-2.17
B3LYP /6-311++G(d,p)	SMD	0.804	0.60	-2.24
B3LYP /6-31+G(d)	CPCM	0.834	0.59	-2.03
B3LYP /6-311++G(d,p)	CPCM	0.834	0.54	-2.03
ωB97XD/6-31+G(d)	SMD	0.787	0.63	-2.11
ωB97XD /6-311++G(d,p)	SMD	0.796	0.61	-2.17
ωB97XD /6-31+G(d)	CPCM	0.818	0.59	-1.98
ωB97XD /6-311++G(d,p)	CPCM	0.790	0.61	-2.16
MN12SX/6-31+G(d)	SMD	0.784	0.64	-2.05
MN12SX /6-311++G(d,p)	SMD	0.814	0.60	-2.26
MN12SX /6-31+G(d)	CPCM	0.820	0.58	-2.00
MN12SX /6-311++G(d,p)	CPCM	0.815	0.59	-2.03

Table S3: Statistics for the quinazoline derivatives training set: R^2, MAD and MAX-ΔpK_a for different DFT methods, basis sets and solvation models using the Q = max{$q(N_1)$, $q(N_3)$} atomic charge descriptor.

DFT/Basis Set	**Solvation Model**	$\mathbf{R^2}$	**MAD**	**MAX-ΔpK_a**
M06L/6-31+G(d)	SMD	0.898	0.47	-1.39
M06L/6-311++G(d,p)	SMD	0.925	0.39	-1.20
M06L/6-31+G(d)	CPCM	0.910	0.44	-1.22
M06L/6-311++G(d,p)	CPCM	0.922	0.41	1.01
M062X/6-31+G(d)	SMD	0.857	0.55	-1.54
M062X /6-311++G(d,p)	SMD	0.882	0.49	-1.34
M062X /6-31+G(d)	CPCM	0.867	0.51	1.61
M062X /6-311++G(d,p)	CPCM	0.903	0.44	-1.20
B3LYP/6-31+G(d)	SMD	0.864	0.52	-1.30
B3LYP /6-311++G(d,p)	SMD	0.889	0.48	-1.47
B3LYP /6-31+G(d)	CPCM	0.888	0.47	1.29
B3LYP /6-311++G(d,p)	CPCM	0.899	0.47	-1.33
ωB97XD/6-31+G(d)	SMD	0.869	0.53	-1.47
ωB97XD /6-311++G(d,p)	SMD	0.891	0.48	-1.38
ωB97XD /6-31+G(d)	CPCM	0.890	0.48	-1.49
ωB97XD /6-311++G(d,p)	CPCM	0.892	0.46	-1.31
MN12SX/6-31+G(d)	SMD	0.853	0.56	-1.58
MN12SX /6-311++G(d,p)	SMD	0.878	0.50	-1.47
MN12SX /6-31+G(d)	CPCM	0.862	0.50	-1.50
MN12SX /6-311++G(d,p)	CPCM	0.891	0.48	-1.32

Table S4: Statistics for the quinazoline derivatives training set: R^2, MAD and MAX-ΔpK_a for different DFT methods, basis sets and solvation models using the Q = min{$q(N_1)$, $q(N_3)$} atomic charge descriptor.

DFT/Basis Set	Solvation Model	R^2	MAD	MAX-ΔpK_a
M06L/6-31+G(d)	SMD	0.862	0.54	-1.44
M06L/6-311++G(d,p)	SMD	0.873	0.52	-1.49
M06L/6-31+G(d)	CPCM	0.885	0.48	-1.42
M06L/6-311++G(d,p)	CPCM	0.863	0.53	1.35
M062X/6-31+G(d)	SMD	0.829	0.59	-1.74
M062X /6-311++G(d,p)	SMD	0.851	0.55	-1.77
M062X /6-31+G(d)	CPCM	0.843	0.57	-1.76
M062X /6-311++G(d,p)	CPCM	0.858	0.52	-1.70
B3LYP/6-31+G(d)	SMD	0.850	0.54	-1.61
B3LYP /6-311++G(d,p)	SMD	0.867	0.52	-1.66
B3LYP /6-31+G(d)	CPCM	0.871	0.53	-1.62
B3LYP /6-311++G(d,p)	CPCM	0.884	0.47	-1.70
ωB97XD/6-31+G(d)	SMD	0.843	0.57	-1.61
ωB97XD /6-311++G(d,p)	SMD	0.861	0.62	-1.21
ωB97XD /6-31+G(d)	CPCM	0.858	0.54	-1.61
ωB97XD /6-311++G(d,p)	CPCM	0.839	0.55	-1.86
MN12SX/6-31+G(d)	SMD	0.824	0.60	-1.70
MN12SX /6-311++G(d,p)	SMD	0.847	0.56	-1.82
MN12SX /6-31+G(d)	CPCM	0.841	0.55	-1.76
MN12SX /6-311++G(d,p)	CPCM	0.846	0.56	-1.75

Table S5: Statistics for the quinazoline derivatives training set: R^2, MAD and MAX-ΔpK_a for different DFT methods, basis sets and solvation models using the Q = avg{$q(N_1)$, $q(N_3)$} atomic charge descriptor.

DFT/Basis Set	**Solvation Model**	**R^2**	**MAD**	**MAX-ΔpK_a**
M06L/6-31+G(d)	SMD	0.899	0.48	-1.17
M06L/6-311++G(d,p)	SMD	0.906	0.43	-1.33
M06L/6-31+G(d)	CPCM	0.923	0.42	-1.08
M06L/6-311++G(d,p)	CPCM	0.904	0.45	1.18
M062X/6-31+G(d)	SMD	0.870	0.53	-1.38
M062X /6-311++G(d,p)	SMD	0.882	0.48	-1.49
M062X /6-31+G(d)	CPCM	0.868	0.47	-1.33
M062X /6-311++G(d,p)	CPCM	0.900	0.43	-1.39
B3LYP/6-31+G(d)	SMD	0.874	0.50	-1.40
B3LYP /6-311++G(d,p)	SMD	0.890	0.47	-1.54
B3LYP /6-31+G(d)	CPCM	0.901	0.47	-1.33
B3LYP /6-311++G(d,p)	CPCM	0.905	0.45	-1.48
ωB97XD/6-31+G(d)	SMD	0.877	0.52	-1.34
ωB97XD /6-311++G(d,p)	SMD	0.888	0.47	-1.49
ωB97XD /6-31+G(d)	CPCM	0.902	0.45	-1.25
ωB97XD /6-311++G(d,p)	CPCM	0.883	0.46	-1.55
MN12SX/6-31+G(d)	SMD	0.862	0.56	-1.37
MN12SX /6-311++G(d,p)	SMD	0.876	0.50	-1.61
MN12SX /6-31+G(d)	CPCM	0.881	0.48	-1.39
MN12SX /6-311++G(d,p)	CPCM	0.888	0.47	-1.45

Table S6: Statistics for the quinazoline derivatives training set: R^2, MAD and MAX-ΔpK_a for different DFT methods and solvation models using the 6-311++G(d,p) basis set and ionization energy (I) as descriptor.

DFT	**Solvation Model**	**R^2**	**MAD**	**MAX-ΔpK_a**
M06L	CPCM	0.760	0.68	2.84
M06L	SMD	0.742	0.70	2.81
B3LYP	CPCM	0.660	0.80	3.00
B3LYP	SMD	0.546	0.95	3.20

Table S7: Statistics for the quinazoline derivatives training set: R^2, MAD and MAX-ΔpK_a for different DFT methods and solvation models using the 6-311++G(d,p) basis set and electron affinity (A) as descriptor.

DFT	**Solvation Model**	**R^2**	**MAD**	**MAX-ΔpK_a**
M06L	CPCM	0.893	0.44	1.47
M06L	SMD	0.853	0.59	-1.57
B3LYP	CPCM	0.724	0.75	-1.99
B3LYP	SMD	0.700	0.81	-2.09

Table S8: Statistics for the quinazoline derivatives training set: R^2, MAD and MAX-ΔpK_a for different DFT methods and solvation models using the 6-311++G(d,p) basis set and electrophilicity index (ω) as descriptor.

DFT	**Solvation Model**	**R^2**	**MAD**	**MAX-ΔpK_a**
M06L	CPCM	0.892	0.48	1.13
M06L	SMD	0.850	0.56	-1.30
B3LYP	CPCM	0.726	0.73	-2.01
B3LYP	SMD	0.707	0.80	-2.12

Table S9: Statistics for the quinazoline derivatives training set: R^2, MAD and MAX-ΔpK_a for different DFT methods and solvation models using the 6-311++G(d,p) basis set and chemical hardness (η) as descriptor.

DFT	**Solvation Model**	R^2	**MAD**	**MAX-ΔpK_a**
M06L	CPCM	0.266	1.18	3.67
M06L	SMD	0.142	1.32	3.47
B3LYP	CPCM	0.261	1.23	3.62
B3LYP	SMD	0.171	1.34	3.52

Table S10: Statistics for the quinazoline derivatives training set: R^2, MAD and MAX-ΔpK_a for different DFT methods and solvation models using the 6-311++G(d,p) basis set and chemical potential (μ) as descriptor.

DFT	**Solvation Model**	R^2	**MAD**	**MAX-ΔpK_a**
M06L	CPCM	0.847	0.53	2.31
M06L	SMD	0.829	0.56	2.24
B3LYP	CPCM	0.725	0.74	2.53
B3LYP	SMD	0.640	0.83	2.75

Table S11: Statistics for the quinazoline derivatives training set: R^2, MAD and MAX-ΔpK_a for different DFT methods and solvation models using the 6-311++G(d,p) basis set and $\dot{X} = f^-(N_1)$ electrophilic fukui function as descriptor.

DFT	**Solvation Model**	R^2	**MAD**	**MAX-ΔpK_a**
M06L	CPCM	0.812	0.62	-2.08
M06L	SMD	0.766	0.69	-2.29
B3LYP	CPCM	0.799	0.59	-2.56
B3LYP	SMD	0.773	0.64	-2.39

Table S12: Statistics for the quinazoline derivatives training set: R^2, MAD and MAX-ΔpK_a for different DFT methods and solvation models using the 6-311++G(d,p) basis set and $\dot{X} = f^-(N_3)$ electrophilic fukui function as descriptor.

DFT	**Solvation Model**	**R^2**	**MAD**	**MAX-ΔpK_a**
M06L	CPCM	0.030	1.50	-3.11
M06L	SMD	0.001	1.45	-3.36
B3LYP	CPCM	0.006	1.49	-3.17
B3LYP	SMD	0.001	1.45	-3.38

Table S13: Statistics for the quinazoline derivatives training set: R^2, MAD and MAX-ΔpK_a for different DFT methods and solvation models using the 6-311++G(d,p) basis set and $\dot{X} = \max\{f^-(N_1), f^-(N_3)\}$ electrophilic fukui function as descriptor.

DFT	**Solvation Model**	**R^2**	**MAD**	**MAX-ΔpK_a**
M06L	CPCM	0.030	1.50	-3.11
M06L	SMD	0.001	1.45	-3.37
B3LYP	CPCM	0.004	1.48	-3.19
B3LYP	SMD	0.001	1.45	-3.39

Table S14: Statistics for the quinazoline derivatives training set: R^2, MAD and MAX-ΔpK_a for different DFT methods and solvation models using the 6-311++G(d,p) basis set and $\dot{X} = \min\{f^-(N_1), f^-(N_3)\}$ electrophilic fukui function as descriptor.

DFT	**Solvation Model**	**R^2**	**MAD**	**MAX-ΔpK_a**
M06L	CPCM	0.812	0.62	-2.08
M06L	SMD	0.768	0.69	-2.28
B3LYP	CPCM	0.801	0.59	-2.56
B3LYP	SMD	0.774	0.64	-2.39

Table S15: Statistics for the quinazoline derivatives training set: R^2, MAD and MAX-ΔpK_a for different DFT methods and solvation models using the 6-311++G(d,p) basis set and $\dot{X} = \text{avg}\{f^-(N_1), f^-(N_3)\}$ electrophilic fukui function as descriptor.

DFT	Solvation Model	R^2	MAD	MAX-ΔpK_a
M06L	CPCM	0.587	0.91	-2.67
M06L	SMD	0.574	0.94	-2.97
B3LYP	CPCM	0.622	0.84	-3.24
B3LYP	SMD	0.578	0.93	-3.14

Table S16: Statistics for the quinazoline derivatives training set: R^2, MAD and MAX-ΔpK_a for different DFT methods and solvation models using the 6-311++G(d,p) basis set and $\dot{X} = f^+(N_1)$ nucleophilic fukui function as descriptor.

DFT	Solvation Model	R^2	MAD	MAX-ΔpK_a
M06L	CPCM	0.809	0.61	1.81
M06L	SMD	0.787	0.68	-1.59
B3LYP	CPCM	0.833	0.58	1.79
B3LYP	SMD	0.786	0.68	-1.64

Table S17: Statistics for the quinazoline derivatives training set: R^2, MAD and MAX-ΔpK_a for different DFT methods and solvation models using the 6-311++G(d,p) basis set and $\dot{X} = f^+(N_3)$ nucleophilic fukui function as descriptor.

DFT	Solvation Model	R^2	MAD	MAX-ΔpK_a
M06L	CPCM	0.031	1.43	-3.50
M06L	SMD	0.027	1.43	-3.54
B3LYP	CPCM	0.036	1.43	-3.60
B3LYP	SMD	0.042	1.41	-3.66

Table S18: Statistics for the quinazoline derivatives training set: R^2, MAD and MAX-ΔpK_a for different DFT methods and solvation models using the 6-311++G(d,p) basis set and $\dot{X} = \max\{f^+(N_1), f^+(N_3)\}$ nucleophilic fukui function as descriptor.

DFT	**Solvation Model**	**R^2**	**MAD**	**MAX-ΔpK_a**
M06L	CPCM	0.115	1.35	-3.59
M06L	SMD	0.109	1.35	-3.66
B3LYP	CPCM	0.140	1.35	-3.73
B3LYP	SMD	0.146	1.32	-3.74

Table S19: Statistics for the quinazoline derivatives training set: R^2, MAD and MAX-ΔpK_a for different DFT methods and solvation models using the 6-311++G(d,p) basis set and $\dot{X} = \min\{f^+(N_1), f^+(N_3)\}$ nucleophilic fukui function as descriptor.

DFT	**Solvation Model**	**R^2**	**MAD**	**MAX-ΔpK_a**
M06L	CPCM	0.641	0.84	-2.63
M06L	SMD	0.641	0.90	-2.05
B3LYP	CPCM	0.720	0.74	2.28
B3LYP	SMD	0.706	0.80	-2.22

Table S20: Statistics for the quinazoline derivatives training set: R^2, MAD and MAX-ΔpK_a for different DFT methods and solvation models using the 6-311++G(d,p) basis set and $\dot{X} = \text{avg}\{f^+(N_1), f^+(N_3)\}$ nucleophilic fukui function as descriptor.

DFT	**Solvation Model**	**R^2**	**MAD**	**MAX-ΔpK_a**
M06L	CPCM	0.309	1.18	-3.17
M06L	SMD	0.304	1.19	-3.35
B3LYP	CPCM	0.356	1.16	-3.45
B3LYP	SMD	0.392	1.08	-3.46

Table S21: Statistics for the quinazoline derivatives training set: R^2, MAD and MAX-ΔpK_a for different DFT methods and solvation models using the 6-311++G(d,p) basis set and $\dot{X} = \Delta f\,(N_1)$ condensed dual function as descriptor.

DFT	**Solvation Model**	**R^2**	**MAD**	**MAX-ΔpK_a**
M06L	CPCM	0.836	0.58	-1.79
M06L	SMD	0.795	0.66	-2.01
B3LYP	CPCM	0.840	0.53	-2.21
B3LYP	SMD	0.804	0.62	-2.08

Table S22: Statistics for the quinazoline derivatives training set: R^2, MAD and MAX-ΔpK_a for different DFT methods and solvation models using the 6-311++G(d,p) basis set and $\dot{X} = \Delta f\,(N_3)$ condensed dual function as descriptor.

DFT	**Solvation Model**	**R^2**	**MAD**	**MAX-ΔpK_a**
M06L	CPCM	0.007	1.44	-3.43
M06L	SMD	0.018	1.43	-3.53
B3LYP	CPCM	0.015	1.43	-3.54
B3LYP	SMD	0.025	1.42	-3.62

Table S23: Statistics for the quinazoline derivatives training set: R^2, MAD and MAX-ΔpK_a for different DFT methods and solvation models using the 6-311++G(d,p) basis set and $\dot{X} = \max\{\Delta f\,(N_1), \Delta f\,(N_3)\}$ condensed dual function as descriptor.

DFT	**Solvation Model**	**R^2**	**MAD**	**MAX-ΔpK_a**
M06L	CPCM	0.863	0.53	-1.70
M06L	SMD	0.850	0.55	-1.97
B3LYP	CPCM	0.849	0.48	-2.33
B3LYP	SMD	0.840	0.54	-2.22

Table S24: Statistics for the quinazoline derivatives training set: R^2, MAD and MAX-ΔpK_a for different DFT methods and solvation models using the 6-311++G(d,p) basis set and $\dot{X} = \min\{\Delta f\,(N_1), \Delta f\,(N_3)\}$ condensed dual function as descriptor.

DFT	**Solvation Model**	**R^2**	**MAD**	**MAX-ΔpK_a**
M06L	CPCM	0.061	1.39	-3.53
M06L	SMD	0.072	1.39	-3.62
B3LYP	CPCM	0.077	1.36	-3.69
B3LYP	SMD	0.085	1.38	-3.72

Table S25: Statistics for the quinazoline derivatives training set: R^2, MAD and MAX-ΔpK_a for different DFT methods and solvation models using the 6-311++G(d,p) basis set and $\dot{X} = \text{avg}\{\Delta f\,(N_1), \Delta f\,(N_3)\}$ condensed dual function as descriptor.

DFT	**Solvation Model**	**R^2**	**MAD**	**MAX-ΔpK_a**
M06L	CPCM	0.497	1.00	-2.91
M06L	SMD	0.492	1.02	-3.17
B3LYP	CPCM	0.531	0.93	-3.36
B3LYP	SMD	0.533	0.95	-3.30

Table S26: Statistics for the quinazoline derivatives training set: R^2, MAD and MAX-ΔpK_a for different DFT methods and solvation models using the 6-311++G(d,p) basis set and $\dot{X} = s^{(2)}\,(N_1)$ local hyper-softness ($s^{(2)}$) as descriptor.

DFT	**Solvation Model**	**R^2**	**MAD**	**MAX-ΔpK_a**
M06L	CPCM	0.853	0.55	-1.56
M06L	SMD	0.807	0.65	-1.65
B3LYP	CPCM	0.840	0.57	-2.00
B3LYP	SMD	0.805	0.65	-1.83

Table S27: Statistics for the quinazoline derivatives training set: R^2, MAD and MAX-ΔpK_a for different DFT methods and solvation models using the 6-311++G(d,p) basis set and $\dot{X} = s^{(2)}(N_3)$ local hyper-softness ($s^{(2)}$) as descriptor.

DFT	**Solvation Model**	**R^2**	**MAD**	**MAX-ΔpK_a**
M06L	CPCM	0.001	1.45	-3.37
M06L	SMD	0.008	1.44	-3.49
B3LYP	CPCM	0.005	1.44	-3.47
B3LYP	SMD	0.012	1.43	-3.56

Table S28: Statistics for the quinazoline derivatives training set: R^2, MAD and MAX-ΔpK_a for different DFT methods and solvation models using the 6-311++G(d,p) basis set and $\dot{X} = \max\{s^{(2)}(N_1), s^{(2)}(N_3)\}$ local hyper-softness ($s^{(2)}$) as descriptor.

DFT	**Solvation Model**	**R^2**	**MAD**	**MAX-ΔpK_a**
M06L	CPCM	0.883	0.47	-1.58
M06L	SMD	0.872	0.52	-1.48
B3LYP	CPCM	0.857	0.49	-2.07
B3LYP	SMD	0.847	0.52	-1.92

Table S29: Statistics for the quinazoline derivatives training set: R^2, MAD and MAX-ΔpK_a for different DFT methods and solvation models using the 6-311++G(d,p) basis set and $\dot{X} = \min\{s^{(2)}(N_1), s^{(2)}(N_3)\}$ local hyper-softness ($s^{(2)}$) as descriptor.

DFT	**Solvation Model**	**R^2**	**MAD**	**MAX-ΔpK_a**
M06L	CPCM	0.037	1.41	-3.54
M06L	SMD	0.053	1.40	-3.64
B3LYP	CPCM	0.050	1.39	-3.69
B3LYP	SMD	0.060	1.40	-3.74

Table S30: Statistics for the quinazoline derivatives training set: R^2, MAD and MAX-ΔpK_a for different DFT methods and solvation models using the 6-311++G(d,p) basis set and $\dot{X} = \text{avg}\{s^{(2)}(N_1), s^{(2)}(N_3)\}$ local hyper-softness ($s^{(2)}$) as descriptor.

DFT	**Solvation Model**	**R^2**	**MAD**	**MAX-ΔpK_a**
M06L	CPCM	0.521	0.99	-2.74
M06L	SMD	0.510	1.03	-3.04
B3LYP	CPCM	0.537	0.93	-3.35
B3LYP	SMD	0.554	0.95	-3.24

Table S31: Molecule number, experimental pK_a, predicted pK_a by using the linear equation pK_a = -5.714A + 19.061 where A represents the calculated electron affinity, difference between experimental and predicted pK_a values for the training set (M06L/6-311++G(d,p)//CPCM).

Molecule number	**pK_a (exp.)**	**pK_a (pred.)**	**ΔpKa**
1	3.31	3.27	-0.04
3	5.73	6.22	0.49
4	3.20	4.67	1.47
7	2.85	3.85	1.00
8	3.51	4.07	0.56
9	3.12	3.64	0.52
10	3.41	3.40	-0.01
11	3.55	2.43	-1.12
12	3.30	2.33	-0.97
15	5.44	5.44	0.00
16	5.16	5.88	0.72
17	5.33	6.09	0.76
18	5.62	5.81	0.19
21	4.78	4.72	-0.06
22	4.98	4.75	-0.23
23	7.79	7.81	0.02
24	7.82	7.82	0.00
25	8.31	9.07	0.76
26	6.98	6.77	-0.21
27	6.31	5.88	-0.43
28	6.61	6.07	-0.54
29	6.20	6.21	0.01
32	8.88	8.30	-0.58
33	7.91	7.25	-0.66
34	8.98	8.17	-0.81
36	6.62	6.53	-0.09
37	6.40	6.18	-0.22
38	6.28	5.98	-0.30
39	5.88	5.53	-0.35
40	5.54	5.70	0.16

Table S32: Molecule number, experimental pK_a, predicted pK_a by using the linear equation pK_a = -5.714A + 19.061 where A represents the calculated electron affinity, difference between experimental and predicted pK_a values for the test set (M06L/6-311++G(d,p)//CPCM).

Molecule number	**pK_a (exp.)**	**pK_a (pred.)**	**ΔpKa**
2	4.43	4.67	0.24
5	2.40	4.42	2.02
6	3.13	5.54	2.41
13	4.18	-2.75	-6.93
14	4.00	-1.76	-5.76
19	4.54	-1.70	-6.24
20	4.27	-2.34	-6.61
30	6.52	6.26	-0.26
31	5.88	5.20	-0.68
35	6.63	0.43	-6.20
41	5.03	5.46	0.43
42	6.02	5.57	-0.45
43	6.08	3.62	-2.46
44	5.37	3.94	-1.43
45	5.28	3.56	-1.72
46	5.77	5.34	-0.43